Ion guiding accompanied by formation of neutrals in polyethylene terephthalate polymer nanocapillaries: Further insight into a self-organizing process

Z. Juhász, B. Sulik, R. Rácz, S. Biri, R. J. Bereczky, K. Tőkési, and Á. Kövér
Institute of Nuclear Research (ATOMKI), Bem tér 18/c, H-4026 Debrecen, Hungary

J. Pálinkás
Department of Experimental Physics, University of Debrecen, Egyetem tér 1, H-4032 Debrecen, Hungary

N. Stolterfoht
Helmholtz-Zentrum Berlin für Materialien und Energie, Glienickerstr. 100, D-14109 Berlin, Germany
(Received 16 August 2010; published 23 December 2010)

A relatively large yield of neutralized atoms was observed when 3 keV Ar^{7+} ions were guided trough polyethylene terephthalate nanocapillaries. Time and deposited-charge dependence of the angular distribution of both the guided ions and the neutrals was measured simultaneously using a two-dimensional multichannel plate detector. The yield of neutrals increased significantly faster than that of guided ions and saturated typically at a few percent level. In accordance with earlier observations, both the yield and the mean emission angle of the guided ions exhibited strong oscillations. For the atoms, the equilibrium was achieved not only faster, but also without significant oscillations in yield and angular position. A phase analysis of these time dependencies provides insight into the dynamic features of the self-organizing mechanisms, which leads to ion guiding in insulating nanocapillaries.

DOI: 10.1103/PhysRevA.82.062903 PACS number(s): 34.35.+a, 61.85.+p

I. INTRODUCTION

In recent years, increasing interest has been devoted to the guided transmission of ions through insulating capillaries [1–7]. The phenomenon involves the charging up of inner capillary walls, which prevents a significant fraction of the ions getting close to the walls; that is, they mostly preserve their initial charge state during the transmission. This "fully elastic" guiding has been found to be significant in capillaries of different sizes and aspect ratios, made from different insulator materials, in a wide range of impact ion energies and charge states [8–20]. Therefore, it is justified to consider the ion-guiding effect as an example for a self-organizing process. For understanding how such a process develops, the temporal dynamics of the transmission pattern of the guided ions is essential.

Recently, systematic works have been started measuring and analyzing the time evolution of the angular transmission profiles [5,6,21–23]. Pronounced oscillations have been observed in the angular position of the ion-transmission profiles, providing evidence for the formation of temporary charge patches produced in the interior of the capillary besides the primary charge patch created in the entrance region [6]. This finding was in accordance with the results of Monte Carlo calculations [7,24–27]. The temporary patches have been found to be important in the pre-equilibrium period, whereas at equilibrium the ions were transmitted along the capillary axis predominantly by the first patch.

A prospective way for gathering more information about the development of charge patches is to study the dynamic properties of the guided ions and those of charge-exchanging inelastic collisions simultaneously. This can be provided by the measurement of all ions with all charge states, as well as the neutralized atoms.

Various experiments have been performed to study the ions, which leave the capillaries with a lower charge state [1–5,28–36]. The experimental study of neutrals requires more effort so that the available information on neutrals produced in capillaries is less detailed or marginal [5,35–38]. All these experiments show that the total sum of ions transmitted into lower charge states is not more than a few percent of those in the initial charge state. Moreover, the fraction of neutrals has been found to be comparable to the fraction of lower charge states [5,37].

In a recent work, nanocapillaries in Al_2O_3 membranes were investigated by ion-impact, and a significant number of particles was detected with a two-dimensional multichannel plate (MCP) detector, which could be identified as neutrals after electrostatic separation [36]. They were observed at all measured tilt angles. Moreover, in contrast to the guided ions, neutral particles appeared almost instantly when the ion beam hit the sample.

In this work we investigate capillaries in polyethylene terephthalate (PET) polymer foils. The dynamic properties of the ion transmission are studied in detail, extending earlier works [6,23]. In addition, the angular distributions of transmitted ions and neutrals were recorded simultaneously with a two-dimensional, position-sensitive MCP detector. The development of the neutral and the ion transmission is found to be different. Both angular positions and intensities exhibit rich oscillatory structures with closely linked phase relations. The relative phases of the oscillations provide an insight into the guiding mechanism, especially into the dynamics of the charge-up process.

II. EXPERIMENT

The experiment was carried out at the Institute of Nuclear Research of the Hungarian Academy of Sciences (ATOMKI), Debrecen. Transmission of 3 keV Ar^{7+} ions through the PET

polymer capillaries was studied. The ions were provided by an electron cyclotron resonance (ECR) ion source [39], which operated with relatively low (429 V) extraction voltage. The beam was collimated by two diaphragms of 1 mm diameter spaced 20 cm apart before entering the vacuum chamber, where the target sample and the detector were placed. This restricted the maximal beam divergence to $\pm 0.3^\circ$. Typical beam current was about 200 pA during the experiment. The vacuum level was $\sim 5 \times 10^{-7}$ mbar. More details about the experimental arrangement can be found in Ref. [36].

For the present experiments, a PET sample with a capillary density of 4×10^6 cm^{-2} was used. It was prepared at the Ionenstrahllabor (ISL) in Berlin [40] and was used earlier in a series of experiments where the dynamic properties of the guided ion transmission were studied [6,23]. The thickness of the sample was 12 μm and the capillary diameter was 200 nm. The angular spread of the capillary inclination was estimated to be $\sim 0.2^\circ$ full width at half maximum (FWHM), which is significantly smaller than the aspect angle of 1°. The density of the capillaries implies a geometric opening of 0.12%. Gold was evaporated under 30° inclination angle on both the front and the back sides of the PET foil, forming a film of $\sim$20 nm thickness to avoid a macroscopic charge up of the sample surfaces.

The target foil was mounted on a sample holder, which allowed for the alignment in three axial dimensions and around one rotational axis. Thus, the horizontal tilt angle ψ of the capillaries could be varied in order to change the angle relative to the incident beam. The vertical (azimuthal) capillary inclination could not be varied. Due to geometric imperfections this azimuthal angle φ with respect to the beam deviated from the ideal 0°. Its value was estimated to be equal to the mean azimuthal angle of the transmitted beam in equilibrium guiding condition with respect to the primary beam, which was found to be $\varphi \approx 0.8^\circ$. The total tilt angle was determined as the root square sum of φ and ψ. For $\psi > 1.8^\circ$ this means only a small correction (<10%). The target foil was mounted on a circular frame with an inner diameter of 7 mm. By moving the sample holder, the beam was localized on a fresh spot in the foil each time when a new measurement with a different tilt angle was started. Hence, previous charge-up effects could be avoided.

The transmitted ions and neutrals were observed using an MCP detector positioned 74 mm away from the target with its sensitive surface parallel with respect to the capillary foil. It was rotated around the same axis as the sample holder by the angle θ_s, whenever ψ was changed. Thus, the angle θ_s was set equal to ψ and the capillary axes always pointed to the same spot in the center of the detector. Two-dimensional images were collected in sequences with an acquisition time of 9 s and a 1 s break between them. The integrated beam current incident on the sample, that is, the deposited charge Q_d, was recorded in each time interval. It was used to normalize the acquired counts. In earlier studies [31,41] it was found that the charging-up dynamics scales with the deposited charge rather than with the time in a wide beam current range. Therefore, the measured quantities were plotted as a function of deposited charge instead of time. Since, however, beam instabilities were small in the present experiment (less than 10%), the deposited charge can also be regarded as a measure of time. Ions were separated from the neutrals by applying an electric field in front of the MCP detector during the whole time when the charge-up dynamics was recorded.

An important aspect of the present work is the measurement of neutrals. The amplitude distribution patterns for the detector signals are different for vacuum ultra-violet (VUV) photons and atoms. In the present measurements only the pattern of Ar atoms with same kinetic energy as the primary beam could be observed. Nevertheless, a small contribution of VUV photons due to radiative transitions of captured electrons cannot be fully excluded [42,43]. However, the photons are emitted in the full solid angle, so that only a minor escape probability through the exit opening is expected, while the scattering of the neutralized atoms is strongly directed toward the capillary exit.

III. EXPERIMENTAL RESULTS AND ANALYSIS

Figure 1 shows an MCP image of the transmitted ions and neutrals acquired after a charge deposition of 150 nC. The positions on the MCP were converted to angular coordinates (θ_x, θ_y). They represent the angular deviations with respect to the beam (z axis) in the x-z and y-z projections. In this case the total tilt angle of the capillaries was equal to 5.5°. The neutrals are emitted in directions close to the capillary inclination. Their position on the MCP was not changed by the electric field, while the ions in the initial charge state (Ar^{7+}) were shifted to the right. Ions with charge states lower than 7 should appear between the positions for Ar and Ar^{7+}. The number of counts, however, was too low to see them as individual peaks.

We determined the transmission yields for Ar and Ar^{7+} by summing the counts within circular areas on the detector surface surrounding the corresponding positions. The radii of the circles were set large enough to include the majority of the signals. Shifting the areas away to signal free positions

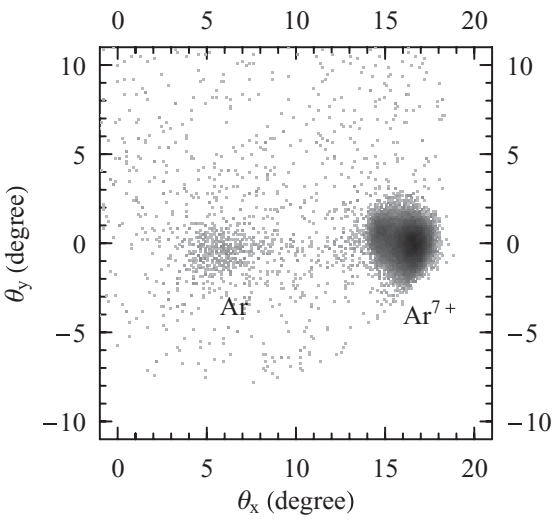

FIG. 1. Two-dimensional angular distribution of the ions transmitted through the capillaries measured by the MCP detector after an amount of 150 nC charge has been deposited on the sample. Ions are separated from neutrals by a horizontal electric field. The capillaries are tilted in the x direction by 5.5°. The neutrals (Ar atoms) appear close to this angle. The ions in the original charge state (Ar^{7+}) are shifted to the right by the separating electric field and appear around $\theta_x = 16^\circ$. The contribution of intermediate charge states is negligible.

the background contribution was determined and subtracted. In order to take into account beam current fluctuations the integrated counts were normalized to the charge deposited at the sample during the acquisition. This process was repeated for each image recorded successively in time. Both the equilibrium states and the time-dependent dynamic effects have been analyzed from the same set of data.

The measurements were performed for several tilt angles from 0.8° to 8°. They essentially show the same features as the example presented here for 5.5°. The capability of insulating capillaries to guide ions is referred to as the guiding power. The fraction of transmitted ions at equilibrium generally decreases exponentially with the square of the tilt angle [2,44]. The guiding power can be quantified by the characteristic guiding angle ψ_c for which the transmission drops to $1/e$ fraction of its value at zero tilt angle [41]. In the present set of measurements we obtained $\psi_c = 5.5°$, which fit well in the scaling law presented in [41].

The tilt angle dependence of the transmission for neutrals was found to be very similar to that of ions. Moreover, we obtained practically the same "guiding angle" $\psi_c = 5.6°$. Under equilibrium conditions ($Q_d > 350$ nC), in the tilt angle range of $\psi = 0.7$–$5.5°$, the neutral-to-ion yield ratio was practically constant, that is, $1.4 \pm 0.1\%$. At $\psi = 8°$ it was somewhat higher, that is, 2.3%. It should be noted that for slow projectiles, the detector sensitivity for the neutral Ar are expected to be lower than for Ar^{7+}; therefore, the real neutral-to-ion ratio could be somewhat larger.

The widths of the angular distributions for the neutrals in both the x and the y direction were found to reach the value of $2.3° \pm 0.2°$ FWHM at 40 nC deposited charge and remained nearly constant during the rest of the charge-up process. For ions, the x width did not stabilize within the measured deposited charge region, while the y width became constant after 100 nC at a value of $1.9° \pm 0.1°$.

Turning to the dynamics of the ion guiding, in Fig. 2, the yields of the detected particles are plotted as the function of deposited charge on the front surface of the target foil Q_d for the capillary tilt angle of 5.5°.

The intensity of transmitted ions is increasing, in accordance with the following approximate function from [6,31]:

$$f(Q_d) = \begin{cases} 0 & \text{if } Q_d < Q_c \\ f_0\left(1 - \exp\left[\frac{Q_d - Q_s}{Q_c}\right]\right) & \text{if } Q_d \geqslant Q_c \end{cases}, \qquad (1)$$

where Q_s is a threshold value and $Q_c$is a characteristic charge constant. Both of them were used as fit parameters.

Figure 2 shows that the first Ar^{7+} ions appeared after the threshold chare of $Q_s = 13$ nC had been deposited on the capillary foil. The fit resulted in a characteristic charge constant of $Q_c = 118$ nC. Similar values were previously obtained for Ne^{7+} ions [6] with similar beam conditions.

Here we draw attention to a remarkable dynamic feature of the guiding mechanism, that is, the clear oscillatory deviation from the exponential function (1), as seen in Fig. 2. This is discussed later. In Ref. [6], indications of such intensity oscillations have also been found.

The intensity of the neutralized Ar atoms increases with the deposited charge as well. The fit by Eq. (1) also appears to be a reasonable approximation. However, a significant

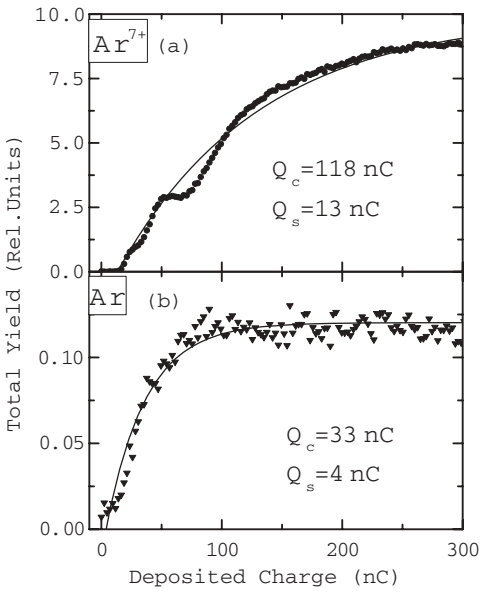

FIG. 2. Total yield of Ar^{7+} (a) and Ar (b) transmitted through the capillaries as function of the deposited charge. The tilt angle of the capillaries was 5.5°. Experimental data are shown as solid symbols. The fit functions (1) are shown as solid lines. The fit parameters Q_c and Q_s are given in the figure.

difference is that, in contrast to the ions, neutrals can be detected immediately after the ion beam is switched on. However, it needs some charge deposition before the intensity starts to increase more rapidly. The fit of the results for the neutrals yields a threshold value of $Q_s = 4$ nC, though the function (1) does not describe so well this early period. For the characteristic charge constant we get $Q_c = 33$ nC, which is significantly smaller than that for the ions. It clearly shows that the emission of neutralized atoms precedes the transmission of guided ions. It is certainly true for the formation of the first patch at the capillary entrance. Note that at such a large tilt angle the immediate appearance of neutrals can be originated only from the entrance region, where ions impinge on the surface.

The mean emission angles of the ions and neutrals were obtained by calculating the first-order moments in θ_x and θ_y over the same circular areas, which had been used for determining the yields. The shifts exerted by the separating electric field to the ions were measured by switching the field on and off, and their effects on the mean emission angle were corrected for. The results are presented in Figs. 3(a) and 3(b). Here, only the components along the x axis (the capillary tilt direction) are shown. We note that Figs. 1, 2, and 3 display data originating from the same measurement.

Closer inspection of Fig. 1 shows that the angular distributions of the Ar^{7+} ions exhibit multiple peak structures in accordance with earlier observations [6,23]. As the charge pattern changes during the charge-up process so does the angular distribution of ions, leading to oscillations of the mean emission angle of ions. In the previous work [6], these characteristic oscillations have already been analyzed, where they were attributed to the formation of temporary charge patches developing in the capillary walls.

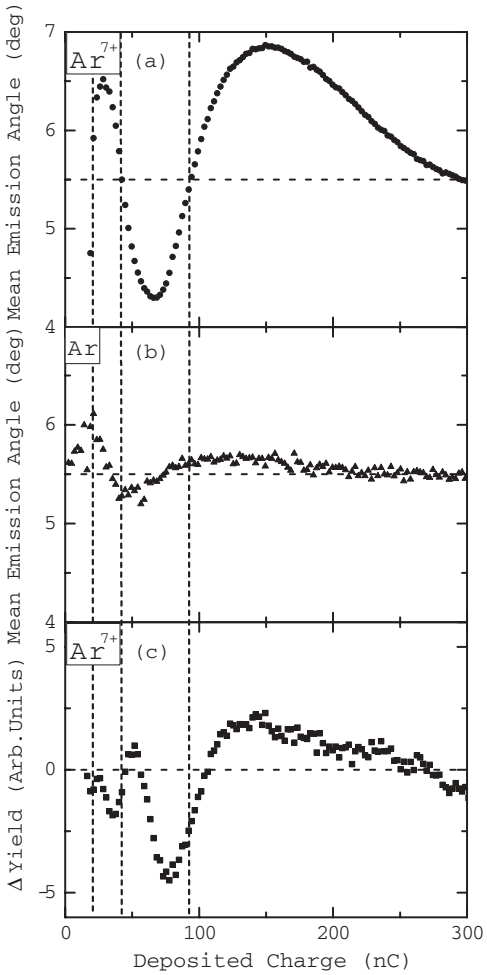

FIG. 3. Mean emission angles of Ar^{7+} (a) and Ar (b) transmitted through the capillaries as function of the deposited charge. The tilt angle was 5.5°. Panel (c) shows oscillatory deviations of the ion intensity from the fit function (1). The crossings of the horizontal (equilibrium) line with the angle oscillations of the ions are marked by dashed lines.

In the case of Ar^{7+} ions the mean emission angle strongly oscillates around the capillary tilt angle. For the neutrals, the oscillation is also present, but with smaller amplitude.

From Figs. 3(a) and 3(b) a characteristic phase relation is readily seen between the two oscillatory patterns; that is, the angular deviation of the neutrals always precedes that of the ions. The first place of maximum deviation of the neutrals coincides with the starting node of the ion position. The node of the neutrals nearly coincides with the maximum deviation of the ions at around $Q_d = 30$ nC, and this node-extremum correspondence continues also for higher values of the deposited charge. Although the oscillation slows down, the phase relation between the two angular position curves remains the same during the whole development. This indicates that not only the first, but all the individual patch formations start with the emission of neutrals.

The amplitude of the angular oscillation for the ions is slightly increasing in the first three half waves, implying that new charge patches temporarily dominate the ion transmission. After the third maximum at around 160 nC, however (i.e., after the formation of the third patch), the angular position of the ion peak smoothly approaches its equilibrium position at the tilt angle of 5.5°. We note that this oscillation pattern is almost identical with that for Ne^{7+} projectiles [6].

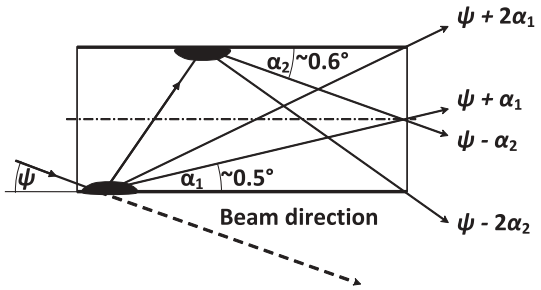

FIG. 4. Schematic view of the formation of the first two patches in a tilted capillary with the characteristic angles for the maximum intensities $(\psi + \alpha_1, \psi - \alpha_2)$ and the maximum angular deviations $(\psi + 2\alpha_1, \psi - 2\alpha_2)$ for ions. Note that for graphical reasons the aspect ratio is strongly reduced and thus angles are enhanced.

The amplitude of the angular oscillation for the neutrals starts with a 0.5° deviation and decreases during the whole period. In contrast to the ions, the emission of neutrals does not seem to be dominated by the new charge patches. Rather, all the formed charge patches seem to contribute to the neutral emission considerably up to the end of the measured period.

In Fig. 3(c) the deviations of the ion yield from the fitting function (1) are shown (in the following referred to as Δ yield), exhibiting more details of the phase relations. The most pronounced of them is that the Δ-yield maxima always appear at around *halfway* (∼20 nC, ∼50 nC, ∼120 nC) to the maximum angular deviation of the ion peak. The Δ-yield minima, appear also regularly at around *halfway back* (∼35 nC, ∼80 nC) from the maximum angular deviation.

To follow these phase relations, we show in Fig. 4 the geometry of the formation of the first and second charge patches in a capillary. It is expected from Fig. 4, that the Δ yield for the detected ions shows its first maximum when the centroid of the angular distribution of the deflected ions aims at the middle of the exit opening at the angle of $\psi + \alpha_1$. After passing this Δ-yield maximum, the mean angular deviation of the ions (from the nominal value of the tilt angle) increases close to its maximum value of $2\alpha_1$ that is geometrically possible. At this maximum angular deviation, however, only a part of the deflected ions reach the capillary exit. A considerable fraction is guided to the opposite side of the capillary, and starts to form the second charge patch. When most of the ions which are deflected by the first patch participate in the formation of the second patch, a minimum appears in the Δ yield.

The formation of the second charge patch looks quite similar to that of the first patch outlined before. The corresponding minima and maxima of the Δ yield and their phase relation to the angular deviation curve can be followed in Fig. 3.

IV. DISCUSSION AND CONCLUSION

From the analysis of the data, we have found that the mean emission angle of the ions oscillates backward and forward by the charge patches formed sequentially at both sides of the capillary wall, as has been explained in Ref. [6]. The present

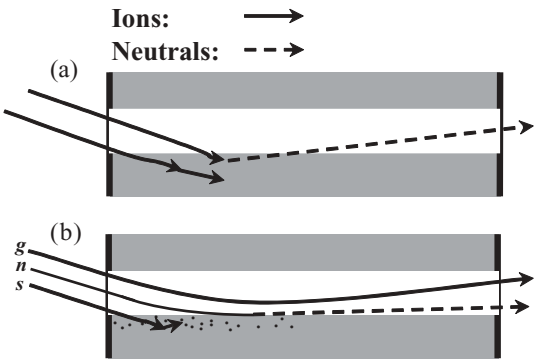

FIG. 5. Tentative scenario for the formation of neutrals in the capillaries. (a) Before charge up, the ions which enter into the surface of the capillary are scattered by the surface layers and neutralized and may escape the capillary. (b) Guiding condition (including equilibrium): scattering, neutralization in a glancing deflection, and distant deflection (guiding) are marked by *s*, *n,* and *g,* respectively.

case of 5.5° tilt angle at 3 keV ion energy shows the formation of three charge patches during the period of the development of the guiding effect.

The patch formation produced a pronounced oscillatory deviation from the exponentially increasing ion intensity. This deviation shows maxima at the deposited charge values, where the ions are deflected by one of the growing charged patches to the direction of the center of the exit opening. The minima of the intensity deviation regularly and closely follow the places for the maximum angular deviations for ions. This can be associated with the formation of the next charge patch at the opposite side of the capillary.

Neutrals occurred immediately after the beam entered the capillaries. Their intensity increased rapidly and reached saturation much earlier than that of the ions. There is a remarkable dependence between the yields of neutrals and ions, namely, that the neutrals reach their equilibrium, when the oscillation in the Δ yield shows its last minimum in Fig. 3(c). This is likely the point where the third (and last) charge patch is being developed and starts to deflect the ions to the capillary exit. This indicates that the sources of neutrals are the charge patches in the capillary wall and the development of neutrals stabilizes when the last patch starts deflecting ions.

In an earlier work, the possibility of the emission of neutrals from the capillary exit was considered [5]. In the present work we found that neutral emission originates dominantly from the entrance and the intermediate regions of the capillaries. Neutralization of the guided ions at the exit of the capillaries is not expected to contribute considerably to neutral emission.

A likely scenario of formation of charge patches that governs the ion guiding and neutral emission based on our present observations is schematically shown in Fig. 5, and is described as follows. At tilt angles as large as 5.5°, the formation of the first charge deposition takes a rather long time. At the beginning, all incoming ions hit the surface of the capillary. Neutralization starts above the surface by capturing the electrons of the insulating material [45]. The projectiles partially penetrate into the bulk and suffer a large angle scattering with atomic cores, whereby they are neutralized. Due to the large angle scattering their escape probability from the capillary is low, but it may result in the weak neutral emission already at the beginning.

Later, when the charge patch forms an increasing deflecting field, more and more ions hit the surface at grazing angle. Some of them are deflected without collisions with the surface. The trajectories of such glancing deflections have sufficiently long contact with the surface that charge exchange occurs quite effectively. When the turning point remains below the critical distance [46], where electron capture processes dominate, ions become fully neutralized, without a significant energy loss. The majority of the neutralized atoms directed toward the capillary exit are formed in this above-the-surface neutralization process.

Soon after that, the first charge patch starts to guide a considerable fraction of the incoming ions. In this state, some of the incoming ions suffer hard collisions, lose their charge, and compensate the discharge currents (see, e.g., the trajectory marked by ***s*** in Fig. 5). Other ions are deflected at a large distance from surface toward the inner part and the exit of the capillary (trajectory marked by ***g*** in Fig. 5). These ions keep their initial charge state and contribute to the guided ion transmission. Henceforward, however, ions deflected on intermediate trajectories are expected to contribute to the formation of neutrals (trajectory marked by ***n*** in Fig. 5).

The formation of the other charge patches developed inside the capillary are expected to be similar. We note that in equilibrium, the first charge patch always plays a key role in guiding and needs a supply of ions for compensating the discharge current. However, the other patches, formed inside the capillary, may change their role or lose their importance during the development of the guiding process.

A remarkable property of the studied dynamics is that some of the parameters, which are characteristic for the emission of neutrals, become constant relatively early. Both the horizontal and the vertical widths of the peak of neutrals stop changing at a value of the deposited charge as small as 40 nC. At 80 nC the intensity of the neutrals reaches saturation. On the contrary, the yield of the guided ions and the mean angular positions approach an equilibrium state only at or above 300 nC. The early stabilization of the width of neutrals suggests that neutrals are emitted dominantly within a narrow (grazing) angular range. This can explain why the contributions from the later formed charge patches do not widen the peak of neutrals at an observable level.

Neutrals have an important property. Since they are not deflected by electric fields along their way to the capillary exit, they directly report on the places, where they were formed. Therefore, the early saturation of the neutral emission is a remarkable finding, which needs further exploratory work.

In summary, two-dimensional angular distributions of the guided ions and the created neutrals were measured for transmission of Ar^{7+} ions through PET polymer capillaries. The charge-up dynamics was studied at several tilt angles by means of the total intensities and the mean emission angles of both the ions and the emitted neutrals. The deposited charge (or time) dependence of the measured yields and angular positions exhibited rich structures. A relatively large yield of neutrals was found in comparison to that of lower charge state ions, which were below the detection limit.

The interpretation of the present experimental findings is in good accordance with the picture based on earlier experimental works and model calculations, but it goes beyond their level due to the simultaneously measured intensity and angular results for guided ions and neutrals and their phase relations.

The main conclusion of the present work is that for any charge depositions, which contribute to the guiding effect, the emission of neutrals occurs before the appearance of the guided ions; that is, *the patch formation always starts with the emission of neurals.* We outlined a scenario for the patch formation, which includes both neutral emission and ion guiding. This picture is supported by the phase relations between the yields and angular positions of the transmission profiles for ions and neutrals. We expect that the findings of the present study provide useful information for future experimental and theoretical work.

ACKNOWLEDGMENTS

This work received partial support from the Hungarian National Science Foundation OTKA (Grant No. K73703). The authors are grateful to Gy. Hegyesi, I. Valastyán and J. Molnár (staff of Department of Electronics of ATOMKI) for constructing the data-acquisition system for the MCP detector.

[1] N. Stolterfoht, J.-H. Bremer, V. Hoffmann, R. Hellhammer, D. Fink, A. Petrov, and B. Sulik, Phys. Rev. Lett. **88**, 133201 (2002).
[2] N. Stolterfoht, V. Hoffmann, R. Hellhammer, Z. D. Pešić, D. Fink, A. Petrov, and B. Sulik, Nucl. Instrum. Methods B **203**, 246 (2003).
[3] M. B. Sahana, P. Skog, Gy. Víkor, R. T. Rajendra Kumar, and R. Schuch, Phys. Rev. A **73**, 040901(R) (2006).
[4] S. Mátéfi-Tempfli *et al.*, J. Pálinkás, and N. Stolterfocht, Nanotechnology **17**, 3915 (2006).
[5] Y. Kanai, M. Hoshino, T. Kambara, T. Ikeda, R. Hellhammer, N. Stolterfoht, and Y. Yamazaki, Phys. Rev. A **79**, 012711 (2009).
[6] N. Stolterfoht, R. Hellhammer, D. Fink, B. Sulik, Z. Juhász, E. Bodewits, H. M. Dang, and R. Hoekstra, Phys. Rev. A **79**, 022901 (2009).
[7] K. Schiessl, W. Palfinger, K. Tőkési, H. Nowotny, C. Lemell, and J. Burgdörfer, Phys. Rev. A **72**, 062902 (2005).
[8] N. Stolterfoht, R. Hellhammer, P. Sobocinski, Z. D. Pešić, J. Bundesmann, B. Sulik, M. B. Shah, K. Dunn, J. Pedregosa, and R. W. McCullough, Nucl. Instrum. Methods B **235**, 460 (2005).
[9] T. Ikeda, Y. Kanai, T. M. Kojima, Y. Iwai, T. Kambara, and Y. Yamazaki, Appl. Phys. Lett. **89**, 163502 (2006).
[10] R. J. Bereczky, G. Kowarik, F. Aumayr, and K. Tőkési, Nucl. Instrum. Methods B **267**, 317 (2009).
[11] M. Kreller, G. Zschornack, and U. Kentsch, J. Phys.: Conf. Ser. **163**, 012090 (2009).
[12] N. Stolterfoht, R. Hellhammer, Z. Juhász, B. Sulik, V. Bayer, C. Trautmann, E. Bodewits, A. J. de Nijs, H. M. Dang, and R. Hoekstra, Phys. Rev. A **79**, 042902 (2009).
[13] G. Sun *et al.*, Phys. Rev. A **79**, 052902 (2009).
[14] Y.-F. Chen *et al.*, Chin. Phys. B **18**, 2739 (2009).
[15] T. Nebiki *et al.*, Nucl. Instrum. Methods B **266**, 1324 (2008).
[16] F. F. Komarov, A. S. Kamyshan, and Cz. Karwat, Vacuum **83**, S51 (2009).
[17] D. H. Li, Y. Y. Wang, Y. T. Zhao, G. Q. Xiao, D. Zhao, Z. F. Xu, and F. L. Li, Nucl. Instrum. Methods B **267**, 469 (2009).
[18] HQ. Zhang, P. Skog, and R. Schuch, J. Phys.: Conf. Ser. **163**, 012092 (2009).
[19] P. Skog, H. Q. Zhang, N. Akram, I. L. Soroka, C. Trautmann, and R. Schuch, J. Phys.: Conf. Ser. **194**, 132030 (2009).
[20] Y. Y. Wang, D. H. Li, Y. T. Zhao, G. Q. Xiao, Z. F. Xu, F. L. Li, and X. M. Chen, J. Phys.: Conf. Ser. **194**, 132032 (2009).
[21] P. Skog, H. Q. Zhang, and R. Schuch, Phys. Rev. Lett. **101**, 223202 (2008).
[22] A. Cassimi *et al.*, Nucl. Instrum. Methods B **267**, 674 (2009).
[23] N. Stolterfoht, R. Hellhammer, D. Fink, B. Sulik, Z. Juhász, E. Bodewits, H. M. Dang, and R. Hoekstra, Nucl. Instrum. Methods B **267**, 669 (2009).
[24] K. Schiessl, W. Palfinger, C. Lemell, and J. Burgdörfer, Nucl. Instrum. Methods B **232**, 228 (2005).
[25] C. Lemell, K. Schiessl, H. Nowotny, and J. Burgdörfer, Nucl. Instrum. Methods B **256**, 66 (2007).
[26] K. Schiessl, W. Palfinger, K. Tőkési, H. Nowotny, C. Lemell, and J. Burgdörfer, Nucl. Instrum. Methods B **258**, 150 (2007).
[27] K. Schiessl, C. Lemell, K. Tőkési, and J. Burgdörfer, J. Phys.: Conf. Ser. **163**, 012081 (2009).
[28] T. Ikeda, T. M. Kojima, Y. Iwai, Y. Kanai, T. Kambara, T. Nebiki, T. Narusawa, and Y. Yamazaki, J. Phys.: Conf. Ser. **58**, 68 (2007).
[29] H. F. Krause, C. R. Vane, and F. W. Meyer, Phys. Rev. A **75**, 042901 (2007).
[30] P. Skog, I. L. Soroka, A. Johansson, and R. Schuch, Nucl. Instrum. Methods B **258**, 145 (2007).
[31] N. Stolterfoht, R. Hellhammer, J. Bundesmann, D. Fink, Y. Kanai, M. Hoshino, T. Kambara, T. Ikeda, and Y. Yamazaki, Phys. Rev. A **76**, 022712 (2007).
[32] X.-M. Chen *et al.*, Chin. Phys. B **18**, 1955 (2009).
[33] G. Kowarik, R. J. Bereczky, F. Aumayr, and K. Tőkési, Nucl. Instrum. Methods B **267**, 2277 (2009).
[34] R. Nakayama, M. Tona, N. Nakamura, H. Watanabe, N. Yoshiyasu, C. Yamada, A. Yamazaki, S. Ohtani, and M. Sakurai, Nucl. Instrum. Methods B **267**, 2381 (2009).
[35] Y. Kanai, M. Hoshino, T. Kambara, T. Ikeda, R. Hellhammer, N. Stolterfoht, and Y. Yamazaki, Nucl. Instrum. Methods B **258**, 155 (2007).
[36] Z. Juhász *et al.*, Nucl. Instrum. Methods B **267**, 321 (2009).
[37] N. Stolterfoht, J. H. Bremer, V. Hoffmann, and D. Fink, *10th International Conference on the Physics of Highly Charged Ions*, Abstract Book (Berkeley, CA, 2000), p. 89.
[38] N. Stolterfoht, R. Hellhammer, Z. D. Pešić, V. Hoffmann, J. Bundesmann, A. Petrov, D. Fink, and B. Sulik, Surf. Coat. Technol. **196**, 389 (2005).

[39] S. Biri, J. Vámosi, A. Valek, Z. Kormány, E. Takács, and J. Pálinkás, Nucl. Instrum. Methods B **124**, 427 (1997).
[40] N. Stolterfoht, R. Hellhammer, J. Bundesmann, and D. Fink, Phys. Rev. A **77**, 032905 (2008).
[41] R. Hellhammer, J. Bundesmann, D. Fink, and N. Stolterfoht, Nucl. Nucl. Instrum. Methods B **258**, 159 (2007).
[42] N. Djurić, J. A. Lozano, S. J. Smith, and A. Chutjian, ApJ **635**, 718 (2005).
[43] J. P. Briand and M. Benhachoum, Nucl. Instrum. Methods B **267**, 665 (2009).
[44] N. Stolterfoht, R. Hellhammer, Z. D. Pešić, V. Hoffmann, J. Bundesmann, A. Petrov, D. Fink, and B. Sulik, Vacuum **73**, 31 (2004).
[45] H. Winter and F. Aumayr, J. Phys. B **32**, 39(R) (1999).
[46] J. Burgdörfer, P. Lerner, and F. W. Meyer, Phys. Rev. A **44**, 5674 (1991).